Inhibition of the matrix metalloproteinase system in a rat model of chronic cyclosporine nephropathy

CARLA DUYMELINCK, JING-TI DENG, SIMONNE E.H. DAUWE, MARC E. DE BROE, and GERT A. VERPOOTEN

Department of Nephrology-Hypertension, University of Antwerp, Antwerp, Belgium

Inhibition of the matrix metalloproteinase system in a rat model of chronic cyclosporine nephropathy.

Background. Chronic cyclosporine A (CsA)-induced nephropathy is histologically characterized by tubular lesions, the interstitial recruitment of inflammatory cells, arteriolopathy and focal interstitial fibrosis. Recent studies show that the intrarenal inhibition of matrix degradation and recruitment of monocytes/macrophages into the kidney plays a critical role in the development of renal interstitial fibrosis.

Methods. We examined the expression of components of the matrix metalloproteinase (MMP) system and plasminogen activator inhibitor type-1 (PAI-1) in kidneys from rats injected daily s.c. during three weeks with CsA (10, 15 or 20 mg CsA/kg body wt) or vehicle solution.

Results. In all CsA-treated rats, serum creatinine levels were significantly elevated compared to control levels. The extent of CsA-induced atrophy was not influenced by the dosage during a three-week CsA treatment. The administration of CsA did not significantly increase total cortical interstitial collagen deposition, whereas α-smooth muscle actin expression was significantly increased in all CsA-treated rats. Analysis of the different subpopulations of inflammatory cells recruited into the chronically injured kidney revealed a marked influx of macrophages into fibrotic cortical foci of CsA-treated rats. The number of cortical macrophages was highest in the group receiving the highest CsA dose. PAI-1 antigen, present in proximal tubular lysosomes in kidneys from all experimental groups, stained very intensely in atrophic tubules in CsA-treated rats. Both stromelysin and interstitial collagenase mRNA were expressed in the kidneys of control rats, but their message transcription remained unaltered after CsA treatment. In contrast, the expression of tissue inhibitor of matrix metalloproteinase type 1 (TIMP-1) was significantly increased after CsA treatment. TIMP-1 mRNA was undetectable in renal sections from sodium-depleted vehicle-treated animals using the *in situ* hybridization (ISH) technique. ISH of selected renal sections of CsA-treated rats identified the cells responsible for the increased TIMP-1 message transcription after CsA administration, mainly as interstitial cells and also as visceral and parietal epithelial cells.

Conclusions. These results suggest that the locally increased expression of TIMP-1 rather than a decrease of matrix metallo-protease expression, contributes to the development of CsA-induced focal interstitial fibrosis in the rat.

The long-term use of cyclosporine A (CsA) as an immunosuppressant in several clinical settings is severely limited by the occurrence of chronic nephropathy [1–4], which consists of progressive renal failure, arterial hypertension and proteinuria [4]. Histopathological changes in the kidney comprise the recruitment of inflammatory cells [5], obliterative arteriolopathy, tubular atrophy and interstitial fibrosis [6]. These CsA-induced tubulointerstitial lesions can readily be reproduced in rodents after three to six weeks of CsA administration, provided a sodium-depletion protocol is followed prior to or during CsA treatment [7–13].

Investigation of the molecular events that lead to renal fibrosis in different rodent models reveals three recurrent themes: a marked infiltration of cells of the monocyte/macrophage lineage, an up-regulated expression of the fibrosis-promoting cytokine TGF-β1, and finally, disturbances in matrix turnover caused by increased fibrogenesis and/or decreased fibrolysis [14]. One can perceive chronic CsA-induced renal fibrosis as the result of uncontrolled tissue repair in response to continuous low-dose toxic insults. In response to CsA, activated and/or injured intrinsic renal cells release chemokines, cytokines and peptide growth factors that recruit inflammatory cells into the kidney, initiate the proliferation of fibroblasts and other resident renal cells, and stimulate the release of several factors that promote renal inflammation and interstitial fibrosis. Furthermore, CsA reduces renal blood flow through the release of vasoactive substances such as thromboxane and endothelin, and the resulting renal ischemia promotes the synthesis of matrix proteins [15]. In addition, CsA directly stimulates renal scarring by increasing collagen production [16] and by increasing the synthesis of transcription factors that promote TGF-β gene transcription [17]. In normal tissue repair processes, immune cell

and fibroblast activity are eventually repressed, cytokine/chemoattractant release returns to baseline, the inflammatory process is terminated, the provisional matrix is resolved and replaced by normal organ tissue. However, repeated insults to the kidney triggered by long-term CsA administration even in low doses can create a chronic, vicious circle of cytokine and matrix overproduction that ultimately leads to progressive interstitial fibrosis.

The interstitial matrix deposited in the scarred kidney is produced by resident cells including activated fibroblasts, recruited mononuclear cells and tubular epithelial cells with a fibrogenic phenotype [18]. Renal matrix degradation is largely regulated by two proteolytic systems that share many features: the matrix metalloproteinase (MMP) system and the plasminogen activating (PA) system. To date 16 vertebrate MMPs have been identified, which are loosely classified into four groups according to protein sequence and substrate specificity [19]. The first class includes interstitial or fibroblast collagenase that hydrolyses all three α-chains of native interstitial collagens, making them susceptible to degradation by gelatinases and other proteases [20]. Secondly, the gelatinases are thought to play a role in both basement membrane turnover (via collagen IV and V breakdown) and in interstitial matrix turnover (via gelatinolytic activity) [20]. Thirdly, stromelysin-1 (or transin, as it is called in the rat) is capable of degrading collagen types II, IV, and V, gelatins, proteoglycans, fibronectin, casein and laminin [20]. Finally, membrane-type MMPs that possess a transmembrane domain are involved in the activation of proMMPs [19]. MMP-mediated matrix degradation is inhibited by tissue inhibitor of matrix metalloproteinases (TIMPs) of which four mammalian species have been identified [21]. We studied the expression of TIMP-1, which is produced by virtually all mesenchymal tissues including intrinsic glomerular cells (mesangial cells and capillary endothelium) and inflammatory cells such as macrophages and fibroblasts [22]. The plasminogen activating (PA) cascade can be blocked at the level of plasminogen activation by the PA inhibitor PAI-1, which results in the inhibition of all subsequent plasmin-mediated activities such as matrix degradation and proMMP activation [23]. In several models of progressive renal fibrosis, matrix deposition highly exceeds the increases of matrix protein gene transcription. This discrepancy results from decreased matrix degradation, as in most models renal TIMP-1 [14] and PAI-1 [14, 23] gene expression is up-regulated, while the transcription of enzymes of the MMP and PA cascade remains unaltered or decreases.

In the present study, we investigated the dose-dependent effects of CsA on renal injury, on the recruitment of inflammatory cells into the renal interstitium and on fibrillar collagen deposition. Until recently most attention in the investigation of CsA-induced renal fibrosis has been focused on the expression of plasminogen activator inhibitor type-1 (PAI-1) [13, 23]. This is the first report demonstrating that up-regulated TIMP-1 expression, rather than decreased MMP gene transcription, contributes to the development of CsA-induced focal tubulointerstitial fibrosis in the rat.

METHODS

Experimental set-up

The rat model of CsA-induced nephropathy used in this study was previously described [12, 23]. Thirty male Wistar rats, initial weight 200 g (Janssen Pharmaceuticals, Beerse, Belgium), were randomly divided into four treatment groups. During the entire study period, the rats were housed in individual polypropylene cages under temperature-controlled conditions in a constant dark-light cycle. CsA-treated animals were daily injected subcutaneously (s.c.) with CsA (SandImmun® i.v.; Sandoz Pharmaceuticals Company, Basel, Switzerland) during three weeks. Three groups ($N = 8$) were studied receiving following doses: 10, 15 and 20 mg CsA/kg body wt. The control group ($N = 6$) was s.c. injected daily with an amount of vehicle for CsA (Cremophor® EL; Sandoz Pharmaceuticals Company), isovolumetric to the dose given to the 20 mg CsA/kg group. Salt depletion, a necessary constituent of the model [11–13, 23], was induced by feeding the rats a sodium-deficient diet based on AIN-76A (ICN Biomedicals, Brussels, Belgium) during their exposure to CsA or vehicle-solution. In addition, renal sections from a separate experiment were used: salt-depleted male Wistar rats were s.c. injected daily with 15 mg CsA/kg body wt or vehicle-solution for five weeks and injected i.p. two hours before sacrifice with lipopolysaccharide (2 mg LPS/kg body wt; from *E. coli*, serotype 0128:B12; Sigma), which is known to increase plasma PAI-1 levels.

Sample collection

After three weeks of treatment, the rats were sacrificed 24 hours after receiving their last injection. The kidneys were quickly prelevated, decapsulated and rinsed in sterile saline solution. The right kidney was snap-frozen in liquid nitrogen and stored at −80°C until RNA extraction was performed. The left kidney was cut into 1 mm thick transverse slices and processed for further histological analysis using different fixation procedures. Serum samples were taken at the time of sacrifice.

Serum creatinine and cyclosporine A levels

Serum creatinine levels were measured in duplicate using a modified colorimetric Jaffé reaction (Creatinine Merckotest; Diagnostica Merck, Darmstadt, Germany). Serum trough CsA levels were determined with a fluorescence polarization immunoassay with a monoclonal antibody to CsA (TD$_x$/TD$_x$ FL$_x$ Cyclosporine Monoclonal Whole Blood Assay; Abbott, Louvain-La-Neuve, Belgium).

Cyclosporine A-induced morphological lesions

For light microscopy, rat kidney slices were fixed in Dubosq-Brasil's solution (an alcoholic based picroformol fixative consisting of 0.77 g picric acid in an ethanol (400 ml):ddH$_2$O (100 ml):neutral formol 40% (200 ml):acetic acid (150 ml) mixture), embedded in paraffin, sectioned at 4 μm, and stained with periodic acid-Schiff (PAS) reagent. Tubular injuries were analyzed as described earlier [23]. In brief, the percentage of injured (atrophic, dilated, vacuolized) tubules was counted in 2 mm^2 of renal cortex. Additionally, the extent of focal renal fibrosis was evaluated by counting the number of fibrotic foci in the total cortex.

Methacarn (6:3:1 methanol/acetic acid/trichloroethane)-fixed paraffin-embedded tissue was cut into 4 μm sections and mounted on poly-L-lysine coated microscope slides and rehydrated. After incubation with normal goat serum [1/5 in Tris saline buffer (TSB: 10 mM Tris-HCl pH 7.6; 0.9% NaCl; 0.1% Triton X-100 and 0.004% merthiolate)] during 20 minutes, rabbit anti-rat collagen I (1/3000 in TSB), rabbit anti-rat collagen III (1/10000 in TSB) anti-serum (Biogenesis Ltd., Bournemouth, UK) or murine monoclonal anti-α smooth muscle actin directed to an amino-terminal synthetic decapeptide of α-smooth muscle actin (1/30000 in TSB; Sigma BioSciences) was applied and incubated overnight. After washing in TSB, sections were treated with biotinylated goat anti-rabbit antiserum or goat anti-murine antiserum (1/200), followed by the addition of the avidin-biotin peroxidase complex (Vector Laboratories Inc., Burlingame, VT, USA). Color development was performed with 3-amino-9-ethylcarbazole (AEC) as a chromogen in the presence of H$_2$O$_2$. Interstitial collagen deposition and α-smooth muscle actin (α-SMA) stainings were measured morphometrically. In each renal section, stainings were quantified in 20 randomly chosen cortical microscopic fields at low magnification (250$\times$, total surface area evaluated 1.7 mm^2) by means of an image analyzer system (Kontron Elektronik Imaging System KS400, release 2.0, Germany). For the analysis of type I collagen and α-SMA, only the interstitial expression was measured: the strongly stained tunica media of arterioles and arteries were rejected manually from the measurement frames. The measurements were expressed as fractional positive area [defined as: (area above threshold divided by frame area) $*$ 100]. Sections were evaluated without any knowledge of the group affiliation of the individual rat.

Phenotyping of inflammatory cells

Macrophage stainings were performed on methacarn-fixed, paraffin-embedded renal tissue with the ED1 monoclonal antibody (Serotec, Oxford, UK), directed to a cytoplasmic antigen of monocytes and tissue macrophages. ED1 also recognizes dendritic cells [24]. Immunohistochemical detection of lymphocytes was performed on 5 μm renal tissue cryosections prefixed on melting ice during 90 minutes in 4% paraformaldehyde (BDH Chemical Ltd., Poole, UK) buffered with 0.1 M Na-cacodylate pH 7.4 containing 1% CaCl$_2$. The W3/25 monoclonal antibody (Serotec, Oxford, UK) used to detect T-helper cells is directed to the rat CD4-equivalent, but also recognizes macrophages [25]. The OX-8 monoclonal antibody (Serotec) was used to detect T-suppressor/cytotoxic and natural killer cells, and is directed to the rat CD8-equivalent [26]. B lymphocytes were counted in sections stained with the OX-4 monoclonal antibody (Harlan Sera-Lab Ltd., Sussex, UK), which recognizes the Ia marker, present on B cells and dendritic cells [27]. Polymorphonuclear neutrophils were identified in hematoxylin eosin stained sections.

Infiltration was quantified as described for a previous CsA nephropathy model [23]. In brief, cells showing distinct immunoreaction were counted in 28 randomly chosen areas (magnification $\times$200; total surface area evaluated per rat, 12 mm^2) in the cortex. Thirty glomerular profiles per renal section were examined for infiltrating cells. Inflammatory cells contained within large blood vessels or surrounded by erythrocytes were excluded from all counts. Results are expressed as absolute numbers of immunoreactive cells per mm^2 or per glomerular cross section. Sections were evaluated without knowledge of the group affiliation of the individual rat.

Cellular proliferation

PAS sections immunostained for the proliferating cell nuclear antigen (PCNA [28]) using the PC10 monoclonal antibody (DAKO, Denmark) were used to evaluate cellular proliferation and to localize proliferating cells. All PCNA-positive nuclei within 16 randomly selected cortical microscopic fields were counted (magnification $\times$200; cortical area evaluated per rat, 7 mm^2). Proliferation was examined separately in intact tubules, in damaged tubules, in glomeruli and in the renal cortical interstitium. At least 40 glomerular cross sections were evaluated per rat. Results were expressed as absolute numbers of PCNA-positive cells per mm^2 cortex or per glomerular cross section. Sections were evaluated without knowledge of the group affiliation of the individual rat.

Combined PCNA/ED1 immunohistochemical staining

To assess for intrarenal macrophage proliferation a microwave-based two color immunohistochemical technique was used [29]. Methacarn-fixed paraffin-embedded renal sections were labeled with ED1 and incubated with biotinylated anti-mouse IgG, avidin and biotinylated alkaline phophatase, after which chromogenic detection was performed with nitroblue tetrazolium salt (NBT) and 5-bromo-4-chloro-3-indolyl phosphate (BCIP) in the presence of L-bromotetramisole. Before applying the second monoclonal antibody, the primary and secondary antibody from the first staining (ED1) were eliminated by microwave heating (2 $\times$ 5 min) in 0.01 M Na-citrate pH 6.0. The second

staining was performed using PC10, followed by incubation in the presence of secondary biotinylated horse anti-mouse immunoglobulins and avidin. Color development was achieved with AEC in 0.01% H_2O_2.

Immunohistochemical staining for PAI-1

Renal tissue fixed on melting ice during 90 minutes in 4% paraformaldehyde (BDH Chemical Ltd., Poole, UK) buffered with 0.1 M Na-cacodylate pH 7.4 containing 1% $CaCl_2$ and embedded in paraffin was sectioned at 4 μm, mounted on poly-L-lysine coated slides, deparaffinized, rehydrated and stained for PAI-1 as described earlier for α-SMA and collagen. Unmasking of PAI-1 antigens was performed by trypsin treatment and mouse anti-human PAI-1 monoclonal antibody, MA-7F5 (provided by R. H. Lijnen and Dr. P. Declerck, Center for Molecular and Vascular Biology, Leuven, Belgium) [30] was applied for overnight incubation. Specificity of the primary antibody has been confirmed in previous experiments [23]. To identify immunoreactive PAI-1 cells, immunostaining was combined with PAS stain and the chromogen 3,3′-diaminobenzidene (DAB) was used to visualize antigen-antibody staining.

Northern blot analysis

For Northern blot analysis, total RNA was isolated by the guanidinium thiocyanate procedure [31]. The following cDNA inserts were used as probes: 0.75 kb *Eco*RI cDNA insert of pG4zTIMP for rabbit TIMP-1 [32] (a gift from Dr. D. Edwards, University of West Ontario, Ontario, Canada), 0.8 kb cDNA insert of pCL-1 for rabbit collagenase and 1.2 kb cDNA insert of pSL-2 for rabbit stromelysin [33] (a gift from Dr. Z. Werb, University of California, San Francisco, CA, USA); the 0.3 kb *Pst*I cDNA insert of pSPβact72, containing part of the 3′ untranslated region of β-actin (a gift from Dr. U. Nudel, The Weizman Institute of Science, Israel) [34]; the 1.3 kb cDNA insert of pRc GAP123 for rat glyceraldehyde-3-phosphate dehydrogenase (GAPDH) [35] (a gift from Dr. R. Wu, Cornell University, Ithaca, NY, USA). Total RNA (10 μg) was electrophoresed at 80V through a denaturing 1.2% agarose gel containing 2.2 M formaldehyde. The separated RNA was fixed on positively charged nylon membranes (Hybond-N$^+$ nylon membrane; Amersham International Plc, Amersham, UK) by alkaline vacuum transfer (Vacugene XL blotting unit; Pharmacia LKB Biotechnology, Uppsala, Sweden). After amplification of the plasmids containing the inserts, cDNA probes were prepared according to standard procedures and ^{32}P-labeled by random primed DNA synthesis (Multiprime DNA labeling kit from Amersham International Plc, UK) to a specific activity of approximately 0.5 to 1.10^9 cpm/μg DNA. After overnight prehybridization at 42°C in hybridization solution [5× standard saline citrate (SSC); 0.1% (wt/vol) SDS; 5× Denhardt's solution; 50 mM sodium phosphate pH 7.0; 0.25 mg/ml denatured sonicated salmon sperm DNA and 50% deionized formamide], the labeled probe was added to

hybridize for 24 hours under the same conditions. Stringency of the washes for each probe was determined in preliminary experiments. Finally, blots were exposed to preflashed Fuji HRG autoradiographic film (Fuji, Japan) at −80°C in a film cassette with two intensifying screens. For quantification, hybridization signals of the blots were scanned densitometrically and integrated by a digital imaging system (Datacopy GS+ scanner, Imagecopy 1.10 software; Xerox, USA) and image analyzer system (Kontron Elektronik Imaging System KS400, release 2.0, Germany). Variations in isolation, application, or transfer of total RNA were accounted for by reprobing the blots with a cDNA probe for GAPDH or β-actin.

The transcription of the housekeeping genes GAPDH and β-actin was investigated in kidneys of experimental rats. A mild but significant increase of β-actin mRNA was observed in CsA-treated rats. Since the expression of GAPDH mRNA was constant after CsA treatment with different doses, all mRNA concentrations were expressed in relation to GAPDH mRNA levels.

Riboprobe preparation for in situ hybridization

The plasmid pBSTIMP1 containing full length rat TIMP-1 cDNA (750 bp) inserted into the pBluescript II SK$^+$ phagemid was provided by Dr. A. Okada (Inserm, Illkirch Cedex, France) [36]. The plasmid construct was linearized using the appropriate restriction enzymes (*Hin*dIII for the TIMP-1 antisense riboprobes and *Bam*HI for the sense TIMP-1 RNA probe) and transcribed using bacteriophage RNA polymerases (T3 RNA polymerase for TIMP-1 antisense and T7 RNA polymerase for TIMP-1 sense probe) in the presence of fluorescein-11-UTP to generate fluorescein-labeled antisense and sense riboprobes according to the manufacturer's instructions (RNA color kit; Amersham). Riboprobe integrity and molecular weight were checked on a 0.8% agarose gel and an estimation of RNA probe concentration was made using UV absorption spectrophotometry.

In situ hybridization

For *in situ* hybridization (ISH), selected Dubosq-Brasil's fixed paraffin-embedded sections were dewaxed in toluene, rehydrated through decreasing graded ethanol, rinsed in diethylpyrocarbonate (DEPC)-treated saline and PBS and fixed for 20 minutes in 4% paraformaldehyde at 4°C. After rinsing in DEPC-PBS, the tissue was permeabilized in 5 μg/ml nuclease-free proteinase K (Boehringer Mannheim) for 20 minutes at 37°C, rinsed in DEPC-PBS and post-fixed in 4% paraformaldehyde at 4°C for 20 minutes. After dehydration in increasing graded ethanols, 25 μl hybridization solution (45% deionized formamide, 1× Denhardt's solution, 0.017 M Tris, 9% dextran sulfate, 4.4 mM EDTA, 0.3 M NaCl, 0.5 μg/μl yeast tRNA, 1 mM dithiotreithol) containing fluorescein-labeled RNA probe was added to each slide. Sections were covered with a coverslip and

Table 1. Functional parameters

	CsA dose *mg/kg body wt*				*P* value
	0	10	15	20	
Body weight (*g*) at time of sacrifice	345 ± 11[a]	313 ± 24[b]	271 ± 25	266 ± 19	0.0000
Serum creatinine *mg/dl*	0.41 ± 0.05[a]	0.64 ± 0.15	0.66 ± 0.14	0.62 ± 0.12	0.0038
CsA serum trough levels *ng/ml*	0 ± 0[a]	1761 ± 373[b]	3009 ± 846	3725 ± 1096	0.0001

Results are expressed as mean ± SD. Body weight and serum creatinine levels were analyzed with ANOVA followed by group-to-group comparisons with the post-hoc Student-Newman-Keuls test.

CsA serum trough levels were analyzed with the Kruskal-Wallis ANOVA and Mann-Whitney U test.

[a] *P* < 0.05, significantly different from all three CsA-treated groups

[b] *P* < 0.05, significantly different from the groups receiving a higher CsA dose

incubated overnight in a humidified box at 55°C. After hybridization, the coverslips were removed in 5 × SSC and sections were incubated for 30 minutes in 50% deionized formamide and 2 × SSC at 65°C to inhibit endogenous alkaline phosphatase activity and to remove nonspecifically bound probe. Sections were rinsed in saline Tris-EDTA buffer (NTE) and background was reduced by incubating in 20 μg/ml ribonuclease A (Boehringer Mannheim) for 35 minutes at 37°C. After rinsing in NTE, sections were incubated at 65°C in 50% deionized formamide in 2 × SSC for 30 minutes, and washed for 15 minutes in 2 × SSC at 50°C and for 15 minutes in 0.1 × SSC at 50°C. Hybridized probes were detected according to the manufacturer's instructions using the RNA color kit (Amersham). In short, the detection required an anti-fluorescein antibody conjugated to alkaline phosphatase and a color-substrate solution consisting of NBT and BCIP. After immunostaining, sections were stained with periodic acid-Schiff reagent, counterstained with methyl green and mounted in glycerol/gelatin. To check the specificity of the fluorescein-labeled antisense riboprobes, in each hybridization run, sections were hybridized with the fluorescein-labeled sense RNA probe or incubated in hybridization solution without probe.

Statistical methods

All data are represented as mean ± SD. Differences between groups were investigated with ANOVA followed by group-to-group comparisons with the post-hoc Student-Newman-Keuls test. Non-parametric variables were analyzed with the Kruskal-Wallis ANOVA and Mann-Whitney *U*-test. In all circumstances, *P* < 0.05 was considered to be significant. Statistical analysis was computed using STATISTICA (release 4.3) for MicroSoft Windows.

RESULTS

Functional parameters

There was no mortality during the course of the study. At the start of the treatment, the mean body wt was 242 ± 12 g. At the time of sacrifice, mean body wt in the vehicle-treated group was significantly higher than in the cyclosporine-treated groups (Table 1). The higher the CsA dose, the smaller the weight gain of the animals after three weeks of CsA treatment. Serum creatinine values were significantly increased in all CsA-treated groups compared to the vehicle-treated group (Table 1). There was no difference between the serum creatinine levels of the CsA-dosage groups. CsA serum trough levels were significantly lower in the group that received 10 mg CsA/kg body wt compared to the CsA-treated groups receiving a higher dose (Table 1).

Renal morphology

In our experimental set-up, CsA caused mild focal tubulointerstitial lesions consisting of tubular atrophy, proximal tubular cell vacuolization and the formation of foci of atrophic tubules in inflamed fibrotic cortical tissue (Table 2). In a few of the CsA-treated animals, a portion of the lesions displayed a characteristic striped distribution extending perpendicularly from the cortico-medullary junction. Examination of the total cortex (Table 2) showed that despite a tendency towards an aggravation of CsA-induced tubular lesions after raising the CsA dosage, only the number of tubules with vacuolized epithelium was significantly increased in the group receiving the highest dose. Isovolumetric vacuolization, a nonspecific but highly characteristic lesion of CsA-induced nephropathy, is a dose-dependent tubulotoxic effect, as is clearly demonstrated by our results.

In control rats, collagen I protein was expressed in the tunica media of arteries and arterioles, but collagen I was also deposited to a limited extent in the cortical interstitium. Increasing CsA dosage increased type I collagen immunostaining in zones containing atrophic tubules. However, morphometric analysis of randomly chosen cortical areas revealed no significant increase of collagen type I deposition after CsA treatment (Table 2). The deposition of collagen type III in the adventitia of blood vessels, surrounding glomeruli and tubules in the cortex of control rat kidneys, tended to increase when the rats were treated with high CsA doses, but the increase of collagen III immunostaining did not reach a significant level when

Table 2. Renal histopathological changes after 3 weeks of CsA treatment

	CsA dose *mg/kg body wt*				*P* value
	0	10	15	20	
Histological lesions					
Tubular atrophy	0.2 ± 0.2^a	20.7 ± 10.7	20.2 ± 11.2	28.3 ± 4.9	0.0026
Tubular vacuolization	0.9 ± 1.2^a	7.8 ± 3.9	10.3 ± 4.7	15.7 ± 3.7^b	0.0000
Tubular dilatation	0.8 ± 1.0	3.2 ± 2.6	3.6 ± 2.8	4.2 ± 2.1	0.0829
Number of cortical fibrotic foci	0 ± 0^a	49.0 ± 28.5	41.5 ± 16.9	57.5 ± 19.1	0.0026
Immunohistochemistry					
Fractional positive area for collagen type I	0.94 ± 0.77	1.23 ± 0.21	2.37 ± 2.22	2.00 ± 1.13	0.2483
Fractional positive area for collagen type III	2.31 ± 1.45	2.42 ± 0.91	4.12 ± 1.43	3.87 ± 0.56	0.1405
Fractional positive area for α-SMA	0.08 ± 0.04^a	0.19 ± 0.09	0.19 ± 0.14	0.27 ± 0.12	0.0038

Histological lesions are expressed as percentage of injured tubules (mean $\pm$ SD). Tubular atrophy, number of fibrotic foci and collagen I and α-SMA were analyzed with the Kruskal-Wallis ANOVA and Mann-Whitney U test. All other data were tested with ANOVA followed by group-to-group comparisons with the post-hoc Student-Newman-Keuls test.

[a] $P < 0.05$, significantly different from all CsA-treated groups
[b] $P < 0.05$, significantly different from CsA-treated groups receiving a lower dose

Table 3. Phenotyping of inflammatory cells

	CsA dose *mg/kg body wt*			
	0	10	15	20
Interstitial infiltration				
ED1 positive cells	23.5 ± 10.3^a	179.2 ± 52.4	150.1 ± 84.9	252.0 ± 35.0
W3/25 positive cells	113.4 ± 70.1	51.3 ± 61.0	150.6 ± 67.4	64.8 ± 31.0
OX-4 positive cells	77.3 ± 46.1	123.6 ± 115.6	116.6 ± 74.5	158.1 ± 115.8
OX-8 positive cells	38.7 ± 17.1	26.1 ± 15.9	32.2 ± 6.9	36.8 ± 14.3
Neutrophils	4.4 ± 3.8^b	9.6 ± 4.0	11.9 ± 3.9	8.2 ± 5.4
Inflammatory cells per glomerular cross section				
ED1 positive cells	0.76 ± 0.24^a	2.70 ± 0.51	2.89 ± 1.04	2.75 ± 0.72
W3/25 positive cells	0.25 ± 0.30	0.12 ± 0.15	0.37 ± 0.16	0.12 ± 0.08^b
OX-4 positive cells	0.32 ± 0.31	0.20 ± 0.08	0.36 ± 0.41	0.19 ± 0.14
OX-8 positive cells	0.12 ± 0.07	0.13 ± 0.05	0.19 ± 0.08	0.06 ± 0.03^b
Neutrophils	0.10 ± 0.05	0.15 ± 0.15	0.21 ± 0.07^c	0.38 ± 0.25^c

Results are expressed as number of immunoreactive cells per mm^2 cortical surface area or per glomerular cross section (mean $\pm$ SD). The number of OX-8 positive cells in interstitium and in glomerular cross sections and glomerular ED1 were analyzed with ANOVA followed by group-to-group comparisons with the post-hoc Student-Newman-Keuls test, while all other data were tested with the Kruskal-Wallis ANOVA and Mann-Whitney U test.

[a] $P < 0.05$ significantly different from all CsA-treated groups
[b] $P < 0.05$ significantly different from the group treated with 15 mg CsA/kg body wt
[c] $P < 0.05$ significantly different from controls and from the group receiving 10 mg CsA/kg body wt

random cortical areas were measured morphometrically, due to the focal nature of CsA-induced interstitial fibrosis (Table 2).

In normal rats α-SMA was constitutively expressed by vascular smooth muscle cells in cortical arteries and arterioles. In salt-depleted vehicle-treated animals sparse α-SMA positive interstitial cells were found around Bowman's capsule and in the interstitial space between tubules (Fig. 1A). In renal sections of CsA-treated rats, foci of α-SMA immunostained cells were detected in the peritubular area (Fig. 1B) and around Bowman's capsule in the cortex. The fractional cortical area positive for α-SMA was significantly increased in all CsA-treated rats (Table 2).

Phenotyping of inflammatory cells

Kidneys from vehicle-treated rats contained very few ED1 positive cells (Fig. 2A and Table 3). The number of interstitial ED1 expressing cells in the total cortex was significantly increased after CsA treatment and the highest number of macrophages was found in the group receiving the highest dose (Table 3). In CsA-treated rats macrophages were located in subcapsular fibrotic foci and were sparse in adjacent intact areas (Fig. 2B). CsA also significantly increased the number of ED1 immunoreactive cells within the glomerular tuft (Table 3). The higher number of macrophages was not only due to an increased renal influx in response to CsA, but was also due to proliferation, as some of the interstitial cells were stained for both ED1 and PCNA (Fig. 2C). The W3/25 positive inflammatory cells (T helper cells and macrophages) were abundantly present in kidneys from all rats and were associated with fibrotic foci in CsA-treated rats (although not to the same extent as ED1 positive cells), but their numbers were not increased in the CsA-treated groups compared with the vehicle-treated group. The W3/25 monoclonal antibody, directed to the rat CD4-equivalent, not only recognizes T helper cells
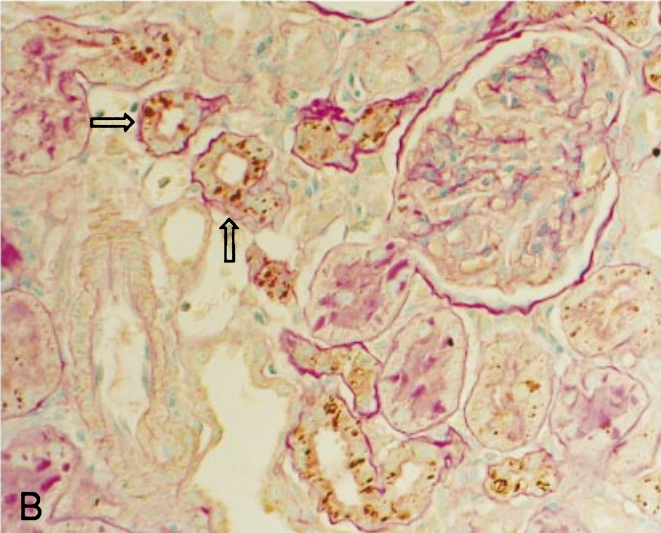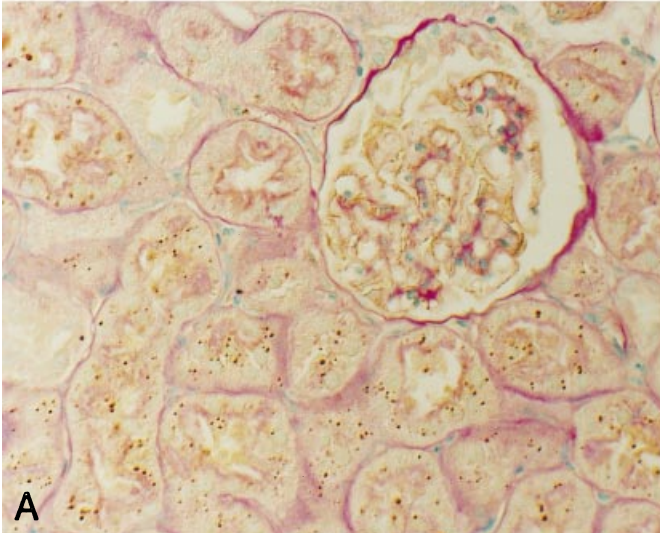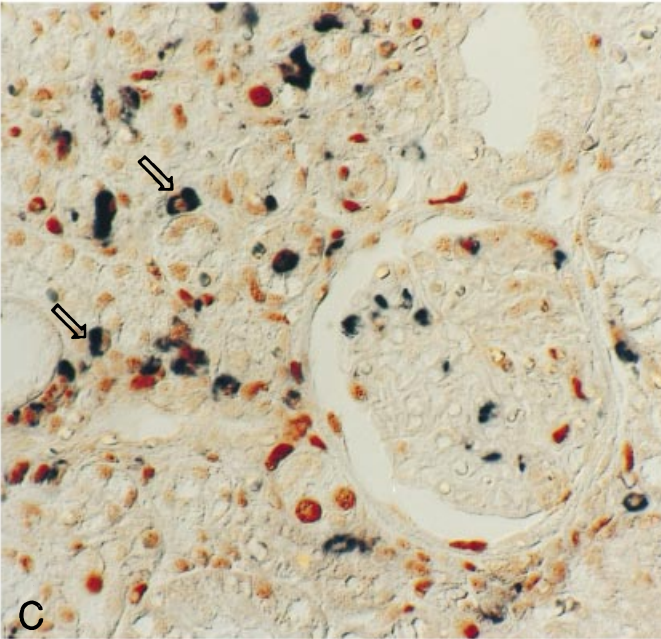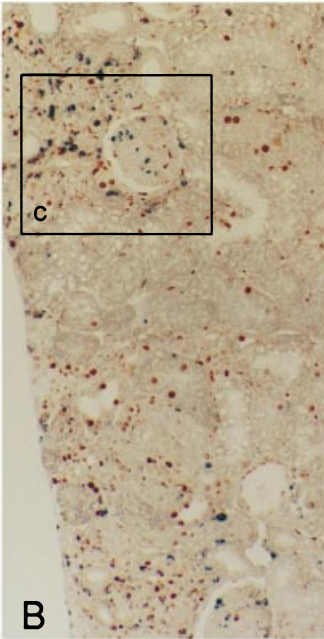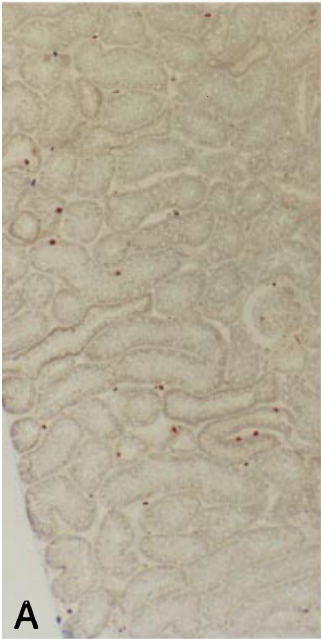
Fig. 1 (upper panels). Immunohistochemical α-smooth muscle actin (α-SMA) staining. (*A*) In the salt-depleted vehicle-treated rat very few interstitial cells are α-SMA positive. (*B*) After CsA treatment (20 mg CsA/kg body wt, 3 weeks) foci of α-SMA expressing interstitial cells are located peritubularly in the subcapsular and deeper cortex. Magnification ×422. The publication of this figure in color was made possible, in part, by a grant from Novartis Pharma Belgium.

Fig. 2 (middle panels). Combined PCNA/ED1 immunohistochemical staining. A microwave-based dual-labeling immunohistochemical technique was used to stain for both proliferating cells (PCNA, brown nuclear staining) and macrophages (ED1, black cytoplasmic staining). (*A*) In kidneys of control rats a limited number of PCNA positive nuclei were found in tubules and in the interstitium. Macrophages were absent. (*B*) In CsA-treated rats (20 mg CsA/kg body wt, 3 weeks) PCNA positive nuclei were associated with focal damaged areas, while adjacent intact areas contained few proliferating cells. Macrophages were even more evidently associated with fibrotic foci. (*C*) Detail of panel B. Cellular proliferation is pronounced in injured (vacuolized, dilated and atrophic) tubules and in the interstitium. Macrophages surround atrophic tubules and infiltrate the glomerular tuft. The increased number of macrophages in CsA-treated rats is not only due to infiltration but also due to proliferation as a subpopulation of macrophages is PCNA positive (arrows). Magnification for A and B ×105; for C, ×422. The publication of this figure in color was made possible, in part, by a grant from Novartis Pharma Belgium.

Fig. 4 (lower panels). Immunohistochemical PAI-1 staining. (*A*) In vehicle-treated sodium-depleted rats, PAI-1 was mainly found in small vesicles (lysosomes) in proximal tubular cells and in visceral epithelium of glomeruli. (*B*) In renal sections of CsA-treated rats (15 mg CsA/kg body wt, 3 weeks) enlarged PAI-1 positive vesicles were observed in atrophic tubules (arrows). Magnification ×338. The publication of this figure in color was made possible, in part, by a grant from Novartis Pharma Belgium.
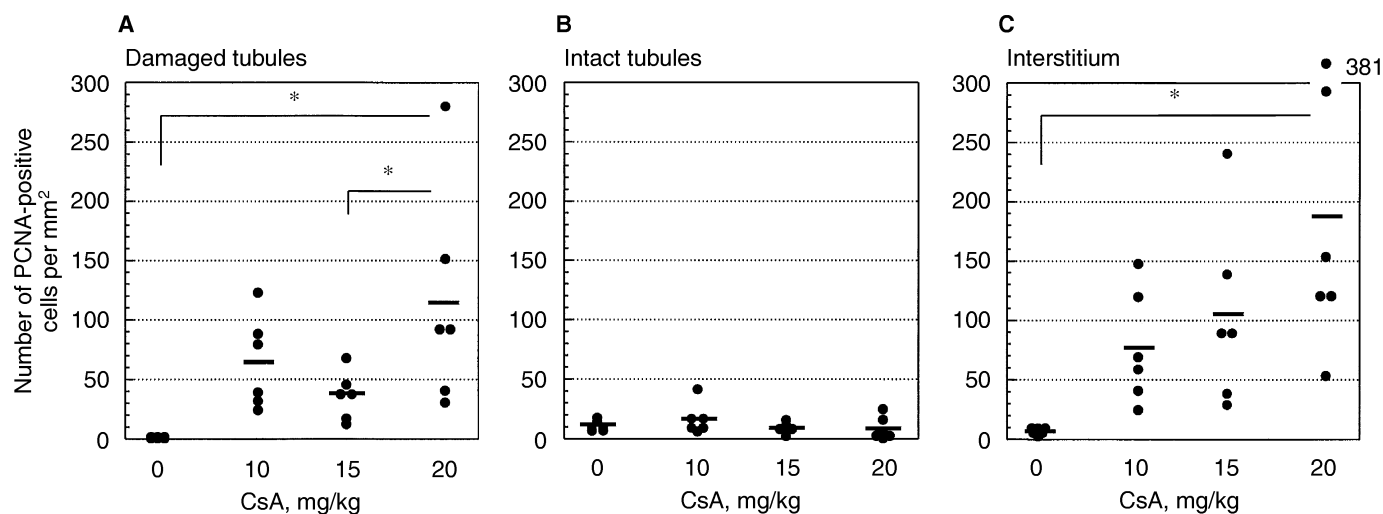

Fig. 3. Quantification of cellular proliferation in the cortex. Proliferation was quantified separately in damaged tubules (atrophy, dilation, vacuolization; *A*), in intact tubules (*B*), in the cortical interstitium (*C*) and in glomeruli. Results are expressed as number of PCNA positive nuclei per mm² cortex. Symbols are: (▬▬▬) mean; (●) individual measurement. *$P < 0.05$. PCNA positivity was much less pronounced in the glomerular compartment: per glomerulus 0.6 ± 0.2; 0.6 ± 0.2; 1.1 ± 0.5 and 2.5 ± 2.0 PCNA positive nuclei were counted in the vehicle-treated, 10, 15 and 20 mg CsA/kg body wt groups, respectively. All data, except PCNA positivity in healthy tubules, were analyzed with ANOVA followed by post-hoc Student-Newman-Keuls testing.

but also macrophages, and probably another interstitial cell type that remains to be identified, which explains the relatively high number of W3/25 immunoreactive cells counted in control rats. In all renal sections B lymphocytes were present in the vicinity of blood vessels, but their recruitment into the kidney was not stimulated by CsA. Cytotoxic T cells and neutrophils were sparse in all experimental groups.

Cellular proliferation

The number of proliferating cells in control rats was negligible (Fig. 2A). PCNA positivity was most pronounced in the interstitial compartment and in injured tubules (that is, atrophic tubules, tubules with a dilated lumen or vacu-

olized epithelial cells) in scarred cortical foci of CsA-treated rats, whereas it was almost absent in adjacent intact areas (Fig. 2). Analysis of randomly chosen cortical fields showed that only the rats receiving 20 mg CsA/kg body wt had significantly higher numbers of PCNA immunoreactive cells in injured tubules, in the cortical interstitium and glomeruli compared to rats receiving vehicle solution (Fig. 3). The lack of significantly increased numbers of PCNA positive nuclei in both groups receiving lower doses is due to the focal nature of the CsA-induced lesions.

Immunohistochemical staining for PAI-1

PAI-1 antigen was immunodetectable in kidneys from all experimental groups. In vehicle-treated salt-depleted rats,
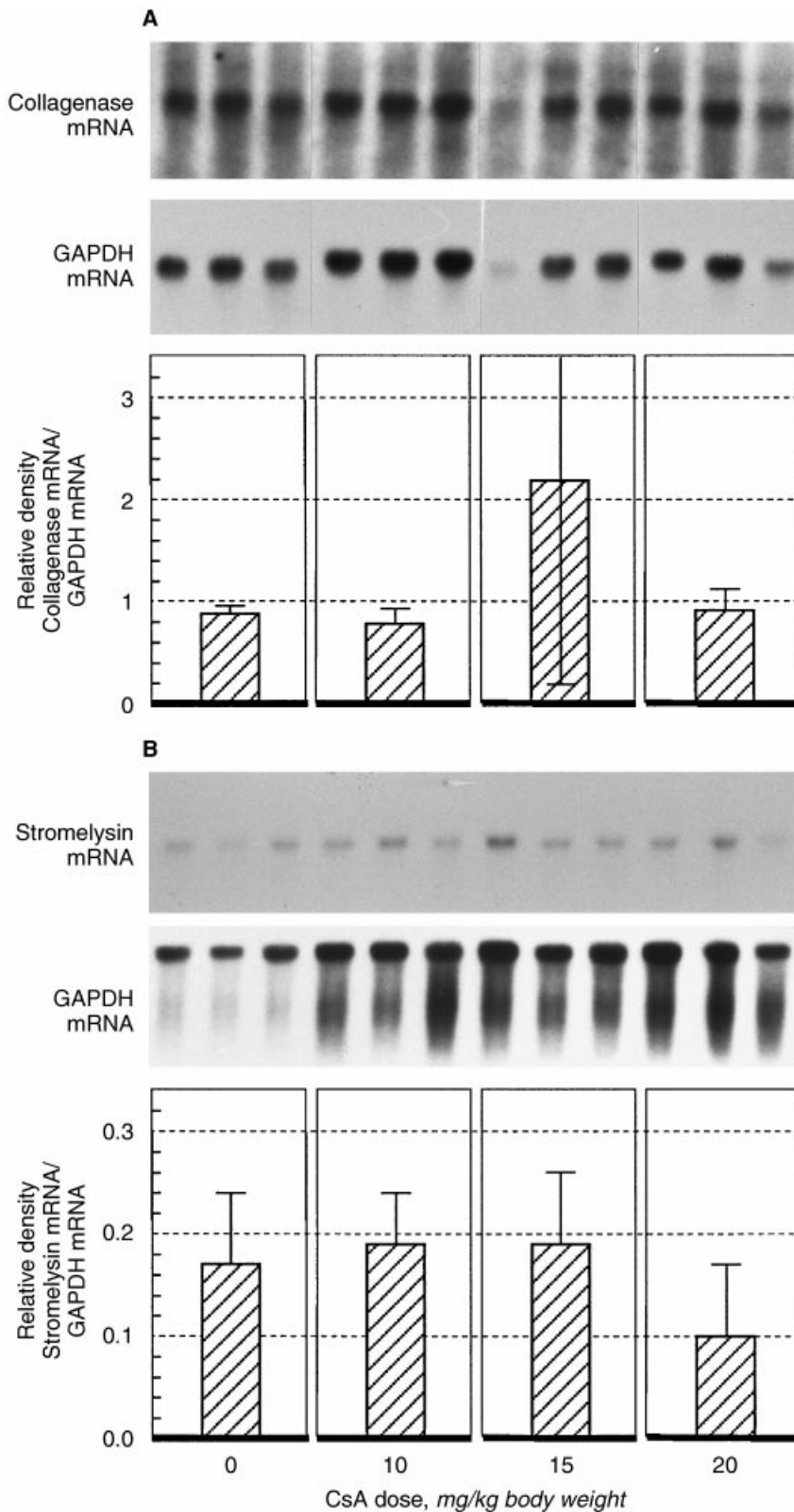
Fig. 5. Northern blot and densitometric analysis of whole kidney RNA for interstitial collagenase (*A*) and stromelysin (*B*) expression. The injected CsA dose is shown under the densitometry graphs. The autoradiograph of GAPDH shows the amount of RNA loaded. Densitometric analyses of the autoradiographs corrected for any RNA loading errors are represented in the bar graphs. Results are expressed as mean ± SD. Data were analyzed with the Kruskal-Wallis ANOVA.

PAI-1 immunoreactive vesicles (lysosomes) were observed in proximal tubular cells (Fig. 4A), mainly in the S1S2 portion of the proximal tubule, and PAI-1 was also found as cytoplasmic staining of arterial smooth muscle and visceral epithelial cells. In addition to these signals in control kidneys, larger and more intensely stained PAI-1 vesicles were present
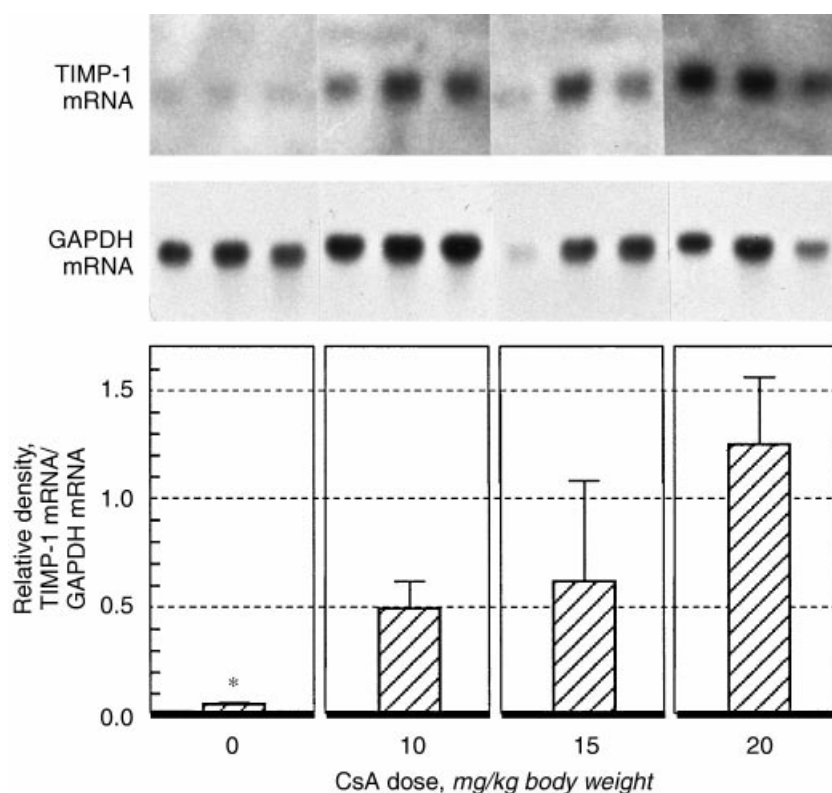
Fig. 6. Northern blot and densitometric analysis of whole kidney RNA for tissue inhibitor of matrix metalloproteinases (TIMP-1) expression. The injected CsA dose is shown under the densitometry graphs. The autoradiograph of GAPDH shows the amount of RNA loaded. Densitometric analysis of the autoradiograph corrected for any RNA loading errors is represented in the bar graphs. Results are expressed as mean ± SD. Data were analyzed with the Kruskal-Wallis ANOVA, and group-to-group comparisons were made with the Mann-Whitney *U*-test (*$P < 0.05$; significantly different from the CsA-treated groups).

in atrophic proximal tubules in damaged cortical foci (arrows, Fig. 4B) in kidneys of rats receiving CsA. PAI-1 immunostaining was comparable in all CsA-treated groups.

Matrix metalloproteinase expression

The rabbit collagenase cDNA probe identified an intense band in control renal rat tissue (Fig. 5A). Low levels of stromelysin transcripts were detected in the kidneys of control rats (Fig. 5B). Normalization for differences in mRNA loading revealed no significant difference between the renal mRNA levels for interstitial collagenase ($P = 0.2165$) and stromelysin ($P = 0.3611$) of the four experimental groups (Fig. 5).

TIMP-1 expression

Only trace amounts of TIMP-1 mRNA could be detected in control kidneys (Fig. 6), but TIMP-1 expression was significantly increased ($P < 0.0329$) in renal tissue from all CsA-treated rats (Fig. 6). The highest TIMP-1/GAPDH ratios were measured in renal RNA extracts derived from rats receiving the highest CsA-dose. A significant linear correlation ($R = 0.833$; $P < 0.001$) was found between the CsA dose and TIMP-1 mRNA expression.

In situ hybridization (ISH) with the hybridization solution lacking an RNA probe, proved that endogenous alkaline phosphatase activity was completely inhibited after the high temperature washes applied in the ISH protocol (data not shown). In sections of animals fed a sodium-deficient diet and treated with vehicle-solution (for 3 or 5 weeks) no TIMP-1 transcribing cells were detected (Fig. 7A). Hybridization of selected sections (of animals treated for 5 weeks with CsA and injected i.p. with LPS 2 hr before sacrifice) with the antisense TIMP-1 RNA probe gave abundant signals in interstitial cells (Fig. 7 B, D). TIMP-1 mRNA transcribing interstitial cells were mainly located in injured areas in peritubular and periglomerular positions, or between inflammatory cells and fibroblasts in the widened interstitial space (Fig. 7 B, D). Parietal and visceral epithelial cells also expressed TIMP-1 message (Fig. 7F) and glomeruli expressing TIMP-1 were located in the injured cortex (Fig. 7B). Some smooth muscle cells of arterioles and arteries were positive for TIMP-1 mRNA. In intact areas TIMP-1 transcribing cells (interstitial or glomerular) were sparse or absent (Fig. 7E). Negative controls to assess aspecific probe adhesion to renal tissue were performed with the TIMP-1 sense riboprobe and gave no signals (Fig. 7C). In sections of control animals receiving a single i.p. injection with LPS two hours before sacrifice, no TIMP-1 mRNA signals could be detected with the ISH technique (data not shown).

DISCUSSION

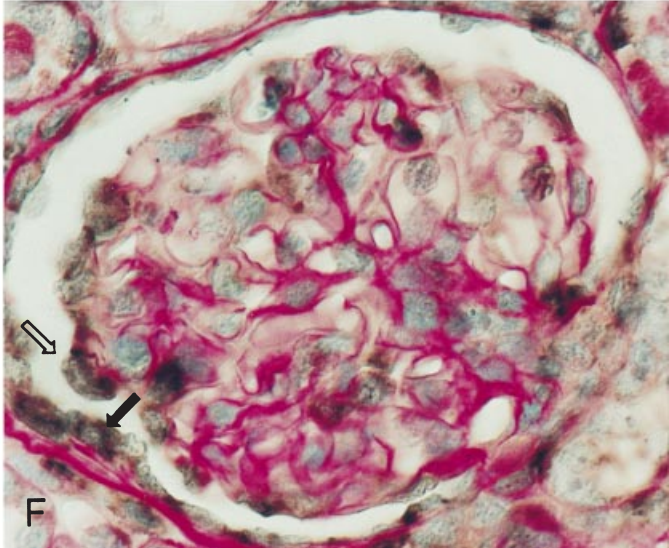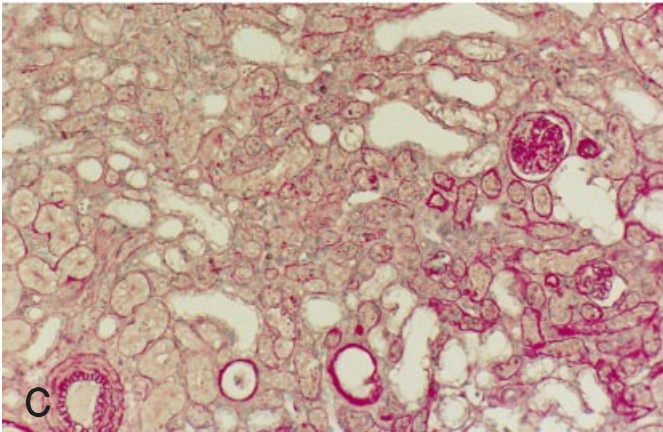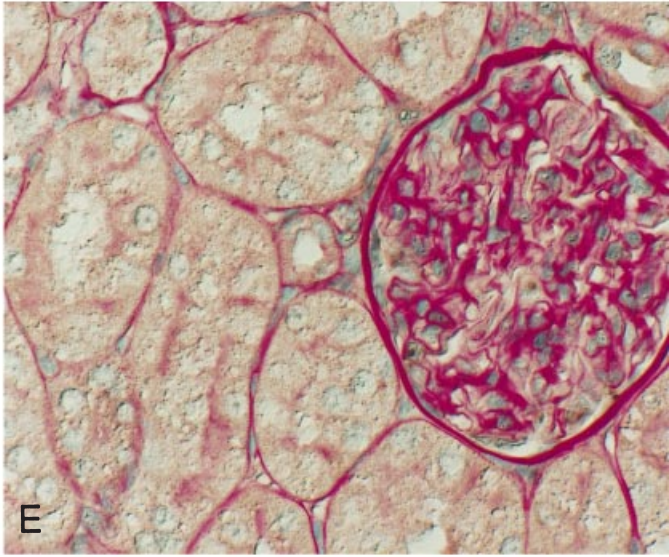We examined the dose-dependent effects of CsA on the expression of fibrosis-related proteins in a model of chronic
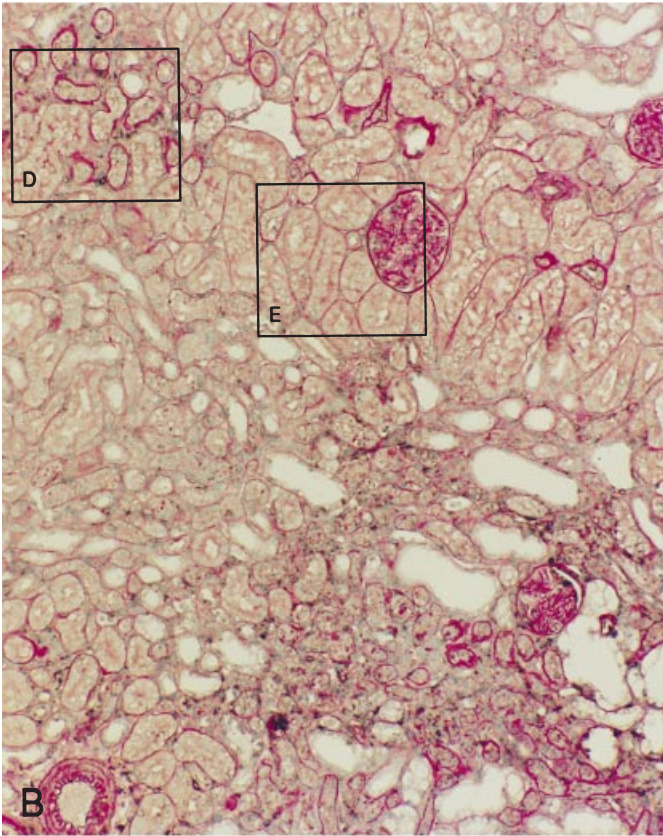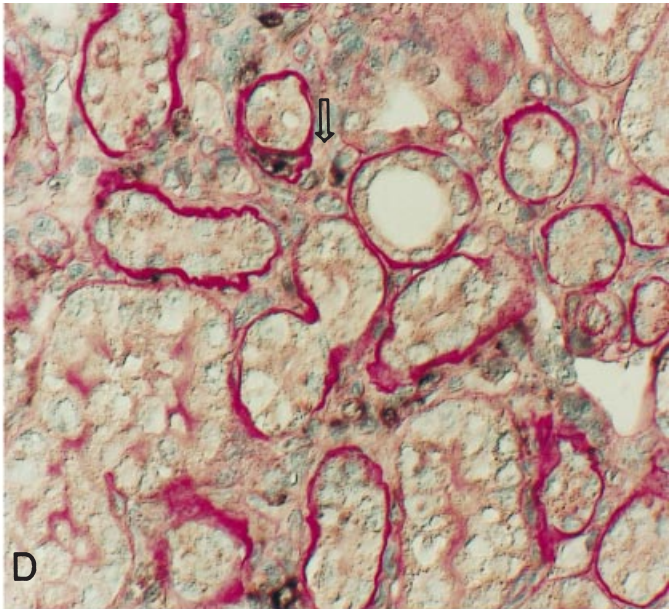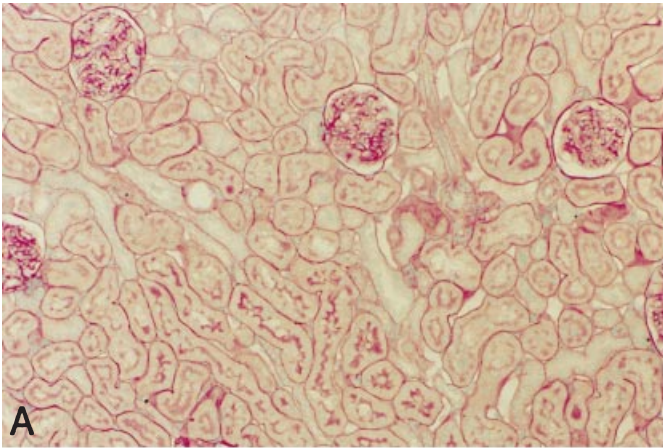
Fig. 7. In situ hybridization (ISH) for TIMP-1 mRNA (A, B, D, E, F) and control hybridization to verify the specificity of the signal (C). (*A*) ISH of kidneys of vehicle-treated salt-depleted rats (3 weeks) with the TIMP-1 antisense probe revealed no TIMP-1 transcribing cells. (*B*) ISH with the antisense TIMP-1 probe of renal sections from CsA-treated rats (15 mg CsA/kg body wt, 5 weeks) shows that interstitial cells in damaged areas are the main site of TIMP-1 gene transcription. TIMP-1 mRNA is also expressed by glomerular cells. (*D*; detail of B) TIMP-1 expressing interstitial cells were mainly present in injured areas in the vicinity of damaged tubules or in the widened interstitial space (arrow). (*E*; detail of B) In adjacent intact areas, TIMP-1 transcribing interstitial and glomerular cells were sparse or absent. (*F*) Glomerular TIMP expressing cells included epithelial cells of Bowman's capsule (black arrow) and visceral epithelial cells (open arrow). (*C*) In each hybridization, consecutive sections were hybridized with sense TIMP-1 riboprobe to assess for aspecific probe adhesion to renal tissue. ISH signals were not observed in any of the negative controls. Magnification A-C, ×105; D, E, ×422; F, ×675. The publication of this figure in color was made possible, in part, by a grant from Novartis Pharma, Belgium.

CsA-induced nephropathy with focal fibrotic lesions, relevant for the study of human CsA-induced renal tubulointerstitial disease. Fibrosis results from increased ECM production and decreased ECM degradation due to decreased protease synthesis and/or increased protease inhibitor expression. In this report we demonstrate that after three weeks of sodium-depletion and CsA administration, the expression of the metalloproteases, interstitial collagenase and stromelysin-1, remained at baseline, while their inhibitor TIMP-1 was overexpressed, adding CsA nephropathy to the growing list of fibrotic nephropathies in which disturbances in the metalloproteinase system are an important feature.

TIMP-1 is a glycoprotein that is produced by virtually all mesenchymal tissues including glomerular cells and inflammatory cells such as macrophages and fibroblasts [22]. TIMP-1 mRNA expressing cells were not detected in kidneys from sodium-depleted rats treated for three or five weeks with vehicle-solution. After five weeks of CsA administration and sodium depletion (and a single LPS injection), TIMP-1 mRNA was transcribed by visceral and parietal epithelium, but most TIMP-1 expressing cells were interstitial. TIMP-1 mRNA positive interstitial and glomerular cells were confined to injured areas. The interstitial cortical cells expressing TIMP-1 message could be resident macrophages or macrophages recruited into the injured areas, fibroblasts and/or resident renal cells that acquired fibrogenic mesenchymal cell characteristics as foci of α-SMA expressing cells were found in the cortex after CsA treatment. In rats injected with a single dose of LPS two hours before sacrifice, no renal TIMP-1 transcribing cells were detected. This may be due to the relative slow on/off transcription kinetics of TIMP-1 [37], but does not exclude an additive stimulatory effect of LPS on TIMP-1 gene expression in CsA-treated rats because *in vitro*, LPS stimulates TIMP-1 synthesis by both monocyte-derived macrophages and their *in vivo* differentiated counterparts [38, 39]. Little is known about the effect of CsA on TIMP-1 expression. The *in vitro* effects of CsA on TIMP-1 expression by human gingival fibroblast strains displays both inter-individual and intra-individual (different strains derived from one individual) heterogeneity [40], and in human dermal fibroblast cultures CsA does not affect TIMP-1 expression [41]. Increased TIMP-1 expression precedes and coincides with fibrogenesis in several rodent renal fibrosis models, but most studies lack information on MMP expression and the identification of the TIMP-1 transcribing cells. In acute puromycin aminonucleoside (PAN) nephrosis, stromelysin expression remains at control values, while TIMP-1 mRNA levels are transiently increased 5-fold at week 1 and collagenase expression increases two- to threefold at weeks 2 and 3 [42, 43]. After sustained injury induced by repeated PAN injections, stromelysin and collagenase expression remain unaltered while TIMP-1 message levels increase for several weeks, and interstitial TIMP-1 immunostaining increases and persists as the interstitial space widens [44]. Focal segmental TIMP deposits appear in glomeruli at a later stage of the disease [44]. Hypercholesteremic uninephrectomized rats develop interstitial fibrosis after 12 weeks, preceded by increased renal TIMP-1 mRNA transcription and the *de novo* interstitial appearance of TIMP-1 protein [45]. In the former two studies, TIMP-1 antigen was stained with rabbit anti-bovine TIMP-1 antiserum [46], which we suspect reacts aspecifically in the rat kidney, since preabsorption of this antiserum to purified bovine TIMP-1 or recombinant human TIMP-1 does not obliterate positive signals, irrespective of the detection method (chromogenic or indirect immunofluorescence) and tissue preparation (unfixed cryostat sections or fixed paraffin-embedded tissue). After unilateral ureteral obstruction of the rat, interstitial fibrosis develops that often evolves to end-stage renal disease. Twelve hours after ureteral ligation TIMP-1 message levels in the obstructed kidney start to rise compared to the levels found in the unobstructed contralateral kidney or kidneys from sham-operated rats [47]. In protein-overload proteinuria induced in uninephrectomized rats by daily bovine serum albumin injections, stromelysin levels remain unaltered during the first three weeks [22]. TIMP-1 mRNA levels are significantly elevated one week after the onset of proteinuria and although interstitial cells are the main site of TIMP gene transcription, some tubular cells contain TIMP-1 message [22]. In the model of passive Heymann nephritis, a transient increase of TIMP-1 gene expression between days 7 and 9 precedes the development of focal interstitial fibrosis [14]. In summary, in several rodent fibrosis models increased TIMP expression appears to be an early event in fibrogenic processes that appears persistent when the renal insult is sustained.

Distinct from its protease inhibitory actions, TIMP-1

displays *in vitro* growth factor activities on epithelial cells and fibroblasts [48, 49]. Specific binding of TIMP-1 to cells sensitive to its growth potentiating effects suggests that these effects are receptor-mediated [48]. A TIMP-induced stimulation of fibroblast proliferation may have significant implications on the matrix-producing potential of the fibrogenic kidney, especially since TIMP-induced growth stimulation of epithelial cells and fibroblasts occurs in the nanomolar range [48]. As other bifunctional molecules such as plasmin, plasminogen activators and the trypsin inhibitor share this growth stimulating activity, there may be an evolutionary link between growth stimulation and regulation of proteolytic activity that has diverged but is still combined in certain proteins [48]. The *in vivo* relevance of the growth factor activities of TIMPs remains to be demonstrated, but in the rat model of chronic CsA nephropathy, tubular and interstitial cell proliferation precedes and coincides with the development of interstitial fibrosis [50], while TIMP-1 expression also appears to be an early event. Further evidence suggesting a possible link between fibrosis and proliferation was put forward by Kuze et al, who demonstrated the increased production of a protein in the remnant kidney that binds to the bidirectional promoter of two collagen IV chains genes and that is also involved in DNA synthesis during replication [51]. In addition, because this protein is nearly identical to the promoter binding protein of the angiotensinogen gene [51], its increased expression may be associated with increased renal levels of angiotensin II, a hormone to which several direct and indirect fibrogenic activities have been ascribed [52].

As described earlier by our group [23], CsA treatment increased PAI-1 lysosomal staining in atrophic tubules located within subcapsular cortical foci, but due to the use of different fixation methods for PAI-1 immunostaining and TIMP-1 ISH, we were unable to determine whether the interstitial TIMP-1 transcribing cells were localized around PAI-1 containing atrophic tubules.

The ability of macrophages to produce fibrosis-inducing cytokines appears to be critical in the progression of tubulointerstitial fibrosis [53–55]. Macrophage depleting protocols ameliorate renal function and reduce the severity of interstitial fibrosis in several models of chronic tubulointerstitial damage [22, 55]. In kidneys from vehicle-treated rats a small population of macrophages resides in the interstitium. Three weeks of CsA treatment significantly increases the number of macrophages in fibrotic areas and macrophage recruitment and/or proliferation appeared to be sensitive to CsA dosage, as the highest numbers of macrophages were encountered in kidneys of rats receiving the highest CsA dose. Monocytes/macrophages are recruited into the renal interstitium in response to several chemoattractants released by tubular cells in response to damage elicited by CsA [54]. The CsA-induced increase of oxidized lipoproteins [56] may also contribute to the recruitment of monocytes into kidneys after CsA-treatment, as oxidized lipoproteins exert chemoattractive activities on monocytes [57]. In addition to recruitment from extrarenal sources, possibly TIMP-1 mediated mitogenic stimuli may lead to interstitial hypercellularity due to macrophage proliferation, as this is partly the case in our model of chronic CsA nephropathy where a small subpopulation of the resident macrophages stain positively for PCNA and since both PCNA positivity and TIMP-1 mRNA expression were highest in the group receiving the highest CsA dose.

The transformation of fibroblasts into myofibroblasts plays a role in tissue repair and renal fibrosis [58]. In control kidneys α-SMA was mainly expressed by vascular smooth cells in cortical arteries and arterioles and α-SMA was absent from the interstitial space except from some rare interstitial α-SMA positive cells lining Bowman's capsule. The focal increase of interstitial α-SMA expression after CsA administration may serve as a predictor of progressive renal dysfunction. In rodent models of progressive renal injury such as urinary outlet obstruction and chronic mesangial proliferative glomerulonephritis, phenotype switching of renal interstitial cells is associated with increased matrix deposition. One of the early pathological events that occur after 5/6 nephrectomy in the rat, is the transformation of renal cells, in which they acquire myofibroblast characteristics [54]. The origin of these myofibroblasts is still controversial; these cells may stem from perivascular cells, vascular smooth muscle cells, resident interstitial fibroblasts [59] or even from tubular cells, since Okada and co-workers found fibroblastic specific protein (FSP1)-positive tubular cells in an inflamed kidney, suggesting a phenotyic conversion of tubular cells into fibroblasts. The very modest interstitial expression of α-SMA after three weeks of CsA treatment indicates that the process of myofibroblast transformation and migration has just begun and may continue to increase as interstitial fibrosis progresses.

The results of our study suggest that the locally increased expression of TIMP-1 in the kidney, rather than a decrease of protease expression, contributes to the development of CsA-induced focal interstitial fibrosis in the rat. The recruitment of macrophages appears to be critical in the progression of CsA-induced tubulointerstitial fibrosis and is affected by CsA dosage since the highest number of macrophages were counted in kidneys of rats treated with 20 mg CsA/kg body wt. The increased TIMP-1 message levels in the fibrotic cortex may be originating from macrophages recruited into injured areas and/or from resident renal cells that acquired fibrogenic mesenchymal cell characteristics, as the number of α-SMA expressing cells increased after three weeks of CsA treatment.

ACKNOWLEDGMENTS

Reprint requests to Gert A. Verpooten, M.D., Department of Nephrology-Hypertension, University of Antwerp, p/a University Hospital Antwerp, Wilrijkstraat 10, B-2650 Edegem/Antwerp, Belgium.
E-mail: VERPOOTE@uia.ua.ac.be

APPENDIX

Abbreviations used in this article are: AEC, 3-amino-9-ethylcarbazole; α-SMA, α-smooth muscle actin; BCIP, 5-bromo-4-chloro-3-indolyl phosphate; CsA, cyclosporine A; DAB, 3,3′-diaminobenzidene; DEPC, diethylpyrocarbonate; FSP1, fibroblastic specific protein; GAPDH, glyceraldehyde-3-phosphate dehydrogenase; ISH, *in situ* hybridization; LPS, lipopolysaccharide; MMP, matrix metalloproteinase; NBT, nitroblue tetrazolium salt; NTE, Tris-EDTA buffer; PA, plasminogen activating; PAI-1, plasminogen activator inhibitor type-1; PAN, puromycin aminonucleoside nephrosis; PAS, periodic acid Schiff; PCNA, proliferating cell nuclear antigen; SSC, standard saline citrate; TGF-β1, transforming growth factor-β1; TIMP-1, tissue inhibitor of matrix metalloproteinase-1; TSB, Tris saline buffer.

REFERENCES

1. MYERS BD, ROSS J, NEWTON L, LUETSCHER J, PERLROTH M: Cyclosporine-associated chronic nephropathy. *N Engl J Med* 311:699–705, 1984

2. PALESTINE AG, AUSTIN HA III, BALOW JE, ANTONOVYCH TT, SABNIS SG, PREUSS HG, NUSSENBLATT RB: Renal pathological alterations in patients treated with cyclosporine for uveitis. *N Engl J Med* 314:1293–1298, 1986

3. YOUNG EW, ELLIS CN, MESSANA JM, JOHNSON KJ, LEICHTMAN AB, MIHATSCH MJ, HAMILTON TA, GROISSER DS, FRADIN MS, VOORHEES JJ: A prospective study of renal structure and function in psoriasis patients treated with cyclosporine. *Kidney Int* 46:1216–1222, 1994

4. MYERS BD, SIBLEY R, NEWTON L, TOMLANOVICH SJ, BOSHKOS C, STINSON E, LUETSCHER JA, WHITNEY DJ, KRASNY D, COPLON NS, PERLROTH MG: The long-term course of cyclosporine-associated nephropathy. *Kidney Int* 33:590–600, 1988

5. PLATT JL, FERGUSON RM, SIBLEY RK, GAJL-PECZALSKA KJ, MICHAEL AF: Renal interstitial cell populations in cyclosporine nephrotoxicity. *Transplantation* 36:343–346, 1983

6. KLINTMALM G, BOHMAN SO, SUNDELIN B, WILCZEK H: Interstitial fibrosis in renal allografts after 12 to 46 months of cyclosporin

treatment: Beneficial effect of low doses in the early post-transplantation period. *Lancet* 2:950–954, 1984

7. GILLUM DM, TRUONG L, TASBY J, MIGLIORI P, SUKI WN: Chronic cyclosporine nephrotoxicity: A rodent model. *Transplantation* 46:285–292, 1988

8. GILLUM DM, TRUONG L, TASBY J: Characterization of the interstitial cellular infiltrate in experimental chronic cyclosporine nephropathy. *Transplantation* 49:793–797, 1990

9. JACKSON NM, HSU C-H, VISSCHER GE, VENKATACHALAM MA, HUMES HD: Alterations in renal structure and function in a rat model of cyclosporine nephrotoxicity. *J Pharmacol Exp Ther* 242:749–756, 1987

10. ROSEN S, GREENFELD Z, BREZIS M: Chronic cyclosporine-induced nephropathy in the rat. *Transplantation* 49:445–452, 1990

11. GERKENS JF, BHAGWANDEEN SB, DOSEN PJ, SMITH AJ: The effect of salt intake on cyclosporine-induced impairment of renal function in rats. *Transplantation* 38:412–417, 1984

12. DENG JT, VERPOOTEN GA, MALESYS J, VERSTREPEN WA, NOUWEN EJ, DE BROE ME: Decreased renal epidermal growth factor expression in cyclosporine-treated rats. *Transplant Proc* 26:2842–2844, 1994

13. SHIHAB FS, TAKESHI FA, TANNER AM, BENNETT WM: Sodium depletion enhances fibrosis and the expression of TGF-β1 and matrix proteins in experimental chronic cyclosporine nephropathy. *Am J Kidney Dis* 30:71–81, 1997

14. EDDY AA: Expression of genes that promote renal interstitial fibrosis in rats with proteinuria. *Kidney Int* 49(Suppl 54):S49–S54, 1996

15. KOPP JB, KLOTMAN PE: Cellular and molecular mechanisms of cyclosporin nephrotoxicity. *J Am Soc Nephrol* 1:162–179, 1990

16. GHIGGERI GM, ALTIERI P, OLEGGINI R, VALENTINI F, GINEVRI F, PERFUMO F, GUSMANO R: Cyclosporine enhances the synthesis of selected matrix proteins by renal cells "in culture." *Transplantation* 57:1382–1388, 1994

17. KHANNA A, KAPUR S, SHARMA V, LI B, SUTHANTHIRAN M: In vivo hyperexpression of transforming growth factor-β1 in mice: Stimulation by cyclosporine. *Transplantation* 63:1037–1039, 1997

18. KUNCIO GS, NEILSON EG, HAVERTY T: Mechanisms of tubulointerstitial fibrosis. *Kidney Int* 39:550–556, 1991

19. NAGASE H: Activation mechanisms of matrix metalloproteinases. *Biol Chem* 378:151–160, 1997

20. DAVIES M, MARTIN J, THOMAS GJ, LOVETT DH: Proteinases and glomerular matrix turnover. *Kidney Int* 41:671–678, 1992

21. KUBOTA T, MATSUKI Y, NOMURA T, HARA K: In situ hybridization study on tissue inhibitors of metalloproteinases (TIMPs) mRNA-expressing cells in human inflamed gingival tissue. *J Periodont Res* 32:467–472, 1997

22. EDDY AA, GIACHELLI CM, MCCULLOCH L, LIU E: Renal expression of genes that promote interstitial inflammation and fibrosis in rats with protein-overload proteinuria. *Kidney Int* 47:1546–1557, 1995

23. DUYMELINCK C, DAUWE SHE, NOUWEN EJ, DE BROE ME, VERPOOTEN GA: Cholesterol feeding accentuates the cyclosporine-induced elevation of renal plasminogen activator inhibitor type 1. *Kidney Int* 51:1818–1830, 1997

24. DIJKSTRA CD, DÖPP EA, JOLING P, KRAAL G: The heterogeneity of mononuclear phagocytes in lymphoid organs: distinct macrophage subpopulations in the rat recognized by monoclonal antibodies ED1, ED2, and ED3. *Immunology* 54:589–599, 1985

25. JEFFERIES WA, GREEN JR, WILLIAMS AF: Authentic T helper CD4 (W3/25) antigen on rat peritoneal macrophages. *J Exp Med* 162:117–127, 1985

26. BRIDEAU RJ, CARTER PB, MCMASTER WR, MASON DW, WILLIAMS AF: Two subsets of rat T lymphocytes defined with monoclonal antibodies. *Eur J Immunol* 10:609–615, 1980

27. MCMASTER WR, WILLIAMS AF: Identification of Ia glycoproteins in rat thymus and purification from rat spleen. *Eur J Immunol* 9:426–433, 1979

28. GARCIA RL, COLTRERA MD, GOWN AM: Analysis of proliferative grade using anti-PCNA/cyclin monoclonal antibodies in fixed embedded tissues. Comparison with flow cytometric analysis. *Am J Pathol* 134:733–739, 1989

29. LAN HY, NIKOLIC-PATERSON DJ, MU W, ATKINS RC: Local macrophage proliferation in the progression of glomerular and tubulointerstitial injury in rat anti-GBM glomerulonephritis. *Kidney Int* 48:753–760, 1995

30. DECLERCK PJ, ALESSI M-C, VERSTREKEN M, KRUITHOF EKO, JUHAN-VAGUE I, COLLEN D: Measurement of plasminogen activator inhibitor 1 in biological fluids with a murine monoclonal antibody-based enzyme-linked immunosorbent assay. *Blood* 71:220–225, 1988

31. CHOMCZINSKY P, SACCHI N: Single step method of RNA isolation by acid guanidinium thiocyanate-phenol-chloroform extraction. *Anal Biochem* 162:156–159, 1987

32. EDWARDS DR, WATERHOUSE P, HOLMAN ML, DENHARDT DT: A growth-responsive gene (16C8) in normal mouse fibroblasts homologous to a human collagenase inhibitor with erythroid-potentiating activity: Evidence for inducible and constitutive transcripts. *Nucl Acids Res* 14:8863–8878, 1986

33. FRISCH SM, CLARK EJ, WERB Z: Coordinate regulation of stromelysin and collagenase genes determined with cDNA probes. *Proc Natl Acad Sci USA* 84:2600–2604, 1987

34. NUDEL U, ZAKUT R, SHANI M, NEUMAN, S, LEVY Z, YAFFE D: The nucleotide sequence of the rat cytoplasmic β-actin gene. *Nucl Acids Res* 11:1759–1771, 1983

35. TSO JY, SUN XH, KAO TH, REECE KS, WU R: Isolation and characterization of rat and human glyceraldehyde-3-phosphate dehydrogenase cDNAs: Genomic complexity and molecular evolution of the gene. *Nucl Acid Res* 13:2485–2502, 1985

36. OKADA A, GARNIER JM, VICAIRE S, BASSET P: Cloning of the cDNA encoding rat tissue inhibitor of metalloproteinase 1 (TIMP-1), amino acid comparison with other TIMPs, and gene expression in rat tissues. *Gene* 147:301–302, 1994

37. LECO KJ, KHOKHA R, PAVLOFF N, HWAKES SP, EDWARDS DR: Tissue inhibitor of metalloproteinases-3 (TIMP-3) is an extracellular matrix-associated protein with a distinctive pattern of expression in mouse cells and tissues. *J Biol Chem* 269:9352–9360, 1994

38. LACRAZ S, NICOD LP, CHICHEPORTICHE R, WELUS HG, DAVER J-M: IL-10 inhibits metalloproteinase and stimulates TIMP-1 production in human mononuclear phagocytes. *J Clin Invest* 96:2304–2310, 1995

39. CAMPBELL EJ, CURY JD, SHAPIRO SD, GOLDBERG GI, WELGUS HG: Neutral proteinases of humans mononuclear phagocytes. Cellular differentiation markedly alters cell phenotype for serine proteinases, metalloproteinases, and tissue inhibitor of metalloproteinases. *J Immunol* 146:1286–1293, 1991

40. LIPTON DA, STRICKLIN GP, DABBOUS MK: Fibroblast heterogeneity in collagenolytic response to cyclosporine. *J Cell Biochem* 46:152–165, 1991

41. LOHI J, KAHARI VM, KESKI-OJA J: Cyclosporin A enhances cytokine and phorbol ester-induced fibroblast collagenase expression. *J Invest Dermatol* 102:938–944, 1994

42. JONES CL, BUCH S, POST M, MCCULLOCH L, LIU E, EDDY AA: Renal extracellular matrix accumulation in acute puromycin aminonucleoside nephrosis in rats. *Am J Pathol* 141:1381–1396, 1992

43. EDDY AA: Protein restriction reduced transforming growth factor β and interstitial fibrosis in nephrotic syndrome. *Am J Physiol* 266:F884–F893, 1994

44. JONES CL, BUCH S, POST M, MCCULLOCH L, LIU E, EDDY AA: Pathogenesis of interstitial fibrosis in chronic purine aminonucleoside nephrosis. *Kidney Int* 40:1020–1031, 1991

45. EDDY AA, LIU E, MCCULLOCH L: Interstitial inflammation and fibrosis in rats with diet-induced hypercholesterolemia. *Kidney Int* 50:1139–1149, 1996

46. DECLERCK YA: Purification and characterization of a collagenase inhibitor produced by bovine vascular smooth muscle cells. *Archiv Biochem Biophys* 265:28–37, 1988

47. ENGELMEYER E, VAN GOOR H, EDWARDS DR, DIAMOND JR: Differential mRNA expression of renal cortical tissue inhibitor of metalloproteinase-1, -2, and -3 in experimental hydronephrosis. *J Am Soc Nephrol* 5:1675–1683, 1995

48. CHESLER L, GOLDE DW, BERSCH N, JOHNSON MD: Metalloproteinase inhibition and erythroid potentiation are independent activities of tissue inhibitor of metalloproteinases-1. *Blood* 86:4506–4515, 1995

49. MURATE T, YAMASHITA K, OHASHI H, KAGAMI Y, TSUSHITA K, KINOSHITA T, HOTTA T, SAITO H, YOSHIDA S, MORI KJ, HAYAKAWA T: Erythroid potentiating activity of tissue inhibitor of metalloproteinases on the differentiation of erythropoietin-responsive mouse erythroleukemia cell line, ELM-I-1–3, is closely related to its cell growth potentiating activity. *Exp Hematol* 21:169–176, 1993

50. YOUNG BA, BURMANN EA, JOHNSON RJ, ALPERS CE, GIACHELLI CM, ENG E, ANDOH T, BENNETT WM, COUSER WG, LINDSEY J, DUYN J: Cellular proliferation and macrophage infiltration precede interstitial fibrosis in cyclosporine nephropathy. *Kidney Int* 48:439–448, 1995

51. KUZE K, SUNAMOTO M, KOMATSU T, IEHARA N, TAKEOKA H, YAMADA Y, KITA T, DOI T: A novel transcription factor is correlated with both glomerular proliferation and sclerosis in the rat renal ablation model. *J Pathol* 183:16–23, 1997

52. SHIHAB FS, BENNETT WM, TANNER AM, ANDOH TF: Angiotensin II blockade decreases TGF-β1 and matrix proteins in cyclosporine nephropathy. *Kidney Int* 52:660–673, 1997

53. ALPERS CE, PICHLER R, JOHNSON RJ: Phenotypic features of cortical interstitial cells potentially important in fibrosis. *Kidney Int* 49(Suppl 54):S28–S31, 1996

54. KLIEM V, JOHNSON RJ, ALPERS CE, YOSHIMURA A, COUSER WG, KOCH KM, FLOEGE J: Mechanisms involved in the pathogenesis of tubulointerstitial fibrosis in 5/6-nephrectomized rats. *Kidney Int* 49:666–678, 1996

55. KOVACS EJ: Fibrogenic cytokines: The role of immune mediators in the development of scar tissue. *Immunol Today* 12:17–23, 1991

56. APANAY DC, NEYLAN JF, RAGAB MS, SGOUTAS DS: Cyclosporine increases the oxidizability of low-density lipoproteins in renal transplant recipients. *Transplantation* 58:663–669, 1994

57. WITZTUM JL, STEINBERG D: Role of oxidized low density lipoprotein in atherogenesis. *J Clin Invest* 88:1785–1792, 1991

58. GRANDE JP: Role of transforming growth factor-β in tissue injury and repair. *Proc Soc Exp Biol Med* 241:27–40, 1997

59. OKADA H, STRUTZ F, DANOFF TM, NEILSON EG: Possible pathogenesis of renal fibrosis. *Kidney Int* 49(Suppl 54):S37–S38, 1996